

SIZE-DEPENDENCE OF THE PHYSICAL AND CHEMICAL PROPERTIES OF COAL FLY ASH*

G. L. Fisher,¹ B. A. Prentice,¹ D. Silberman,¹ J. M. Ondov,²
R. C. Ragaini,² A. H. Bierman,² A. R. McFarland,³ and J. B. Pawley.⁴

¹Radiobiology Laboratory, University of California, Davis, CA 95616

²Lawrence Livermore Laboratory, Livermore, CA 94550

³Civil Engineering Department, Texas A & M University, College Station, TX 77843

⁴Donner Laboratory, University of California, Berkeley, CA 94720

In order to aid in the assessment of the potential biomedical and environmental consequences of coal combustion for electric power generation, we have performed detailed collaborative studies of the physical and chemical properties of size-fractionated coal fly ash. In this report, we demonstrate that many of the physical and chemical properties of aerodynamically size-classified fly ash depend on the relative size distributions of each fraction.

Aerodynamically size-classified fly ash was collected downstream from the electrostatic precipitator (ESP) in the stack breeching of a large southwestern U. S. power plant burning low sulfur (0.5%), high ash (23%) coal. The specially designed collection system (1) which consists of two cyclones and a centripeter separator is capable of size-classifying *in situ* kilogram quantities of stack fly ash. When used for 12 days to collect fly ash from stack gas, the apparatus yielded a total of 8.08 kg of fly ash in fractions with volume median diameters (VMD) of 20 μm (fraction 1), 6.3 μm (fraction 2), 3.2 μm (fraction 3) and 2.2 μm (fraction 4) all with geometric standard deviations of approximately 1.8. The size distribution data determined by optical sizing, centrifugal sedimentation and Coulter analyses are presented in Table 1.

Physical Studies

Based on light microscopic study of the four fly ash fractions, we have developed a particle morphogenesis scheme (Fig. 1). The physical characteristics of opacity, shape and type of inclusion utilized in the morphogenesis scheme appear to be related to degree and extent of exposure of the fly ash to combustion zone temperatures.

Eleven particle types and their probable matrix composition are classified (Fig. 1): 1) amorphous, non-opaque, 2) amorphous, opaque, 3) amorphous, mixed opaque and non-opaque, 4) rounded, vesicular, non-opaque, 5) rounded, vesicular, mixed opaque and non-opaque, 6) angular, lacy, opaque, 7) non-opaque, cenosphere (hollow sphere), 8) non-opaque, plerosphere (sphere packed with other spheres), 9) non-opaque, solid sphere, 10) opaque sphere and 11) non-opaque spheres with either surface or internal crystals. We have quantified the relative abundances of each of the 11 morphologic particle types in the four fractions (Table 2). The relative abundance of all particle types except non-opaque, solid spheres appears to increase with the increasing particle size of the fly ash fractions. The relative abundance of non-opaque, solid spheres is inversely dependent on particle size. Chi-square analyses of the relative distribution data of the morphologic particle types in the four fly ash fractions indicated highly significant ($p < 0.001$) differences for all six possible comparisons.

The apparent densities of the four fractions (Table 2) can be negatively correlated ($r = -0.978$; $p < 0.05$) with the VMD's. Furthermore, linear regression analyses of the fractional distribution data with the densities of the individual size fractions indicate significant ($p < 0.05$) positive correlations for the following particle types: 1) amorphous, non-opaque, 4) rounded, vesicular, non-opaque, 7) non-opaque cenospheres and 10) opaque sphere. Significant negative correlation was found only for solid, non-opaque spheres ($p < 0.01$).

*This work was supported by the US Energy Research and Development Administration.

Chemical Studies

The fly ash fractions were analyzed for 35 elements by instrumental neutron activation analysis (INAA) at the Lawrence Livermore Laboratory and for 18 elements by atomic absorption spectroscopy (AAS) at the Radiobiology Laboratory. The analytical techniques have been previously described (2). Before analyses of the fly ash fractions were undertaken both laboratories performed analyses of the National Bureau of Standards (NBS) Standard Reference Material, Trace Elements in Coal Fly Ash (SRM 1633). Agreement of all analytical results from both laboratories with previously published (3) or NBS certified values was excellent. The interlaboratory comparison has been reported by Ondov *et al.* (2).

Summary tables of the analytical results are presented for those elements displaying concentrations independent of particle size (Table 3) and dependent on particle size (Table 4). For elements analyzed by both INAA and AAS, the data reported are the results of the analytical technique with the smaller coefficient of variation. Data from atomic absorption analyses are the average of two independent determinations; the INAA data are the weighted averages of three independent determinations. Concentration dependence with particle size was determined qualitatively with the criteria that consistent concentration trends beyond experimental uncertainty were observed for each fraction, although significantly higher concentrations of the element may have been observed in the finest fraction relative to the coarsest fraction.

With the exception of silicon, which appears to decrease with decreasing particle size, the major element composition of the fractionated fly ash is relatively independent of particle size. Greater than 92% of the mass of the fractionated fly ash can be accounted for by oxides of Si, Al, Fe and Ca. An enhancement factor was defined as the ratio of the element concentration in cut 4 (finest) to its concentration in cut 1 (coarsest). The more volatile elements (or their oxides), Cd, Zn, Se, As, Sb, Mo, Ga, Pb and V display clear-cut increases in concentration with decreasing particle size, in agreement with the vapor-condensation mechanism of Natusch and Wallace (4). It is important to note, however, that refractory elements also display concentration trends inversely dependent on particle size. Therefore, processes other than vapor condensation are involved in the concentration-size relationship. The elements U and Cr are associated with the organic fraction of coal (5) and may be released in the combustion process as fine particles which may agglomerate with other particles. The elements Fe, Mn, Ba, and Sr (5) may in part be present as carbonate minerals which decompose to form fine particles during coal combustion and again agglomerate with other particles. Copper is probably present in part as the sulfide and Be as the aluminosilicate in the coal (5). Thus, mineral decomposition and elemental distribution may in part explain the elemental trends of the high boiling chemical species.

In summary, many physical and chemical properties of coal fly ash are dependent on particle size. Apparent density varies inversely with particle size and may be explained by the higher relative abundance of vesicular particles and lower relative abundance of solid, non-opaque spheres in larger size fractions. The elements Al, Fe, Ca, Na, K, Ti, Mg, Sr, Ce, La, Rb, Nd, Th, Ni, Sc, Hf, Co, Sm, Dy, Yb, Cs, Ta, Eu and Tb do not display clear-cut concentration trends with particle size. Silicon was the only element analyzed with clear-cut direct concentration dependence with particle size. Inverse concentration dependence with particle size was observed for Cd, Zn, Se, As, Sb, W, Mo, Ga, Pb, V, U, Cr, Ba, Cu, Be and Mn. Although a vapor-condensation mechanism may explain the concentration trends for the volatile elements, mineral decomposition and elemental distribution within the coal are probably important processes contributing to the inverse concentration dependence observed for the higher boiling chemical species.

References

1. McFarland, A. R., Fisher, G. L., Prentice, B. A., Bertch, R. W. Submitted to Environ. Sci. Technol.
2. Ondov, J. M., Ragaini, R. C., Heft, R. E., Fisher, G. L., Silberman, D., Prentice, B. A. Proc. NBS 8th Materials Research Symposium, Gaithersburg, MD. September, 1976, in press.
3. Ondov, J. M., Zoller, W. H., Omez, I., Aras, N. K., Gordon, G. E., Rancitelli, L. A., Abel, K. H., Filby, R. H., Shah, K. R., Ragaini, R. C. Anal. Chem. 47, 1102 (1975).
4. Natusch, D. F. S., Wallace, J. R. Science 186, 695 (1974).
5. Murchison, D., Westoll, T. S. "Coal and coal-bearing strata", 418 pp, American Elsevier, N. Y., 1968.

Table 1. Size Parameters for the Fly Ash Fractions

Fraction	CMD ¹		MMD ²		VMD ³	
	μm	σg ⁴	μm	σg	μm	σg
1	2.73	2.20	18.5	2.8	20.0	1.8
2	2.58	1.86	6.0	2.0	6.3	1.8
3	1.14	1.73	3.7	1.7	3.2	1.8
4	0.92	1.52	2.4	1.8	2.2	1.9

¹Count median diameter determined from scanning electron micrographs.

²Mass median diameter determined from Stokes differential settling in aqueous dispersion.

³Volume median diameter determined by Coulter analysis.

⁴Geometric standard deviation.

Table 2. Relative Abundance (%) of Morphologic Particle Types in the Four Fly Ash Fractions¹

Particle Type	Fraction			
	1	2	3	4
1. Amorphous, non-opaque	7.25	2.13	0.79	0.33
2. Amorphous, opaque	0.42	0.18	--	--
3. Amorphous, mixed opaque and non-opaque	0.77	0.09	--	--
4. Rounded, vesicular, non-opaque	12.39	6.67	2.91	2.99
5. Rounded, vesicular, mixed opaque and non-opaque	2.27	0.24	--	0.03
6. Angular, lacy, opaque	1.34	0.57	0.27	0.33
7. Non-opaque, cenosphere	41.11	26.22	13.20	7.91
8. Non-opaque, plerosphere	0.51	0.21	--	--
9. Non-opaque, solid sphere	25.58	56.01	79.16	86.99
10. Opaque sphere	1.56	0.90	0.33	0.24
11. Non-opaque sphere with crystals	6.80	6.79	3.18	0.95
12. Combined ² particle types 2 and 6	--	--	0.15	0.24
VMD (μm)	20	6.3	3.2	2.2
Density ³ (g/cm ³)	1.85	2.19	2.36	2.45

¹A total of approximately 3000 particles for each size fraction were classified from random fields using three microscope slides per fraction.

²Combined due to inability to distinguish between these classes for the finer particles.

³Apparent density determined by gravimetric displacement of 1-propanol.

Table 3. Elemental Concentrations Independent¹ of Particle Size

Element	Technique	Fraction 1 (VMD = 20 μm)	Fraction 2 (VMD = 6.3 μm)	Fraction 3 (VMD = 3.2 μm)	Fraction 4 (VMD = 2.2 μm)
<u>Concentration in %</u>					
Al	AAS ²	13.8(0.1)	14.4(0.1)	14.2(0.8)	14.1(0.3)
Fe	INAA ³	2.5(0.1)	2.9(0.2)	3.0(0.1)	3.2(0.1)
Ca	AAS	2.12(0.14)	2.23(0.08)	2.30(0.14)	2.38(0.09)
Na	AAS	1.19(0.13)	1.75(0.05)	1.83(0.06)	1.85(0.03)
K	AAS	0.74(0.01)	0.80(0.07)	0.82(0.08)	0.81(0.03)
Ti	AAS	0.62(0.05)	0.76(0.05)	0.77(0.11)	0.78(0.06)
Mg	AAS	0.47(0.01)	0.56(0.01)	0.60(0.02)	0.63(0.01)
<u>Concentration in μg/g</u>					
Sr	INAA	410(60)	540(140)	590(140)	700(210)
Ce	INAA	113(4)	122(5)	123(6)	120(5)
La	INAA	62(3)	68(4)	67(11)	69(3)
Rb	INAA	51(3)	56(4)	57(3)	57(8)
Nd	INAA	45(4)	47(4)	49(7)	52(6)
Th	INAA	25.8(0.6)	28.3(0.6)	29(1)	30(2)
Ni	AAS	25(3)	37(1)	43(4)	40(2)
Sc	INAA	12.6(0.5)	15.3(0.6)	15.8(0.6)	16.0(0.2)
Hf	INAA	9.7(0.4)	10.3(0.3)	10.5(0.3)	10.3(0.5)
Co	INAA	8.9(0.2)	16.3(0.8)	19(1)	21(1)
Sm	INAA	8.2(0.3)	9.1(0.4)	9.2(0.4)	9.7(0.4)
Dy	INAA	6.9(0.3)	8.5(0.9)	8.1(0.3)	8.5(0.8)
Yb	INAA	3.4(0.4)	4.1(0.4)	4.0(0.2)	4.2(0.3)
Cs	INAA	3.2(0.1)	3.7(0.2)	3.7(0.2)	3.7(0.2)
Ta	INAA	2.1(0.1)	2.3(0.2)	2.5(0.3)	2.7(0.1)
Eu	INAA	1.0(0.1)	1.2(0.2)	1.2(0.2)	1.3(0.4)
Tb	INAA	0.90(0.05)	1.06(0.06)	1.10(0.07)	1.13(0.06)

¹Concentration dependence with particle size was determined qualitatively with the criteria that consistent concentration trends beyond experimental uncertainty were observed for each fraction.

²AAS values are the averages of two independent determinations; the ranges are given in parentheses.

³INAA values are the weighted averages of three independent determinations; uncertainties (in parentheses) are the largest of twice the weighted standard deviation, the range, or an estimate of the accuracy.

Table 4. Elemental Concentrations Dependent¹ on Particle Size

Element	Technique	Fraction 1 (VMD = 20 μm)	Fraction 2 (VMD = 6.3 μm)	Fraction 3 (VMD = 3.2 μm)	Fraction 4 (VMD = 2.2 μm)	Enhancement Factor ²
Concentration in μg/g (unless indicated)						
Cd	AAS ³	0.4(0.2)	1.6(0.3)	2.8(0.4)	4.6(0.2)	11.5
Zn	AAS	68(1)	189(4)	301(10)	746(218)	11.
Se	INAA ⁴	19(2)	59(2)	78(2)	198(20)	10.4
As	INAA	13.7(1.3)	56(14)	87(9)	132(22)	9.6
Sb	INAA	2.6(0.1)	8.3(0.4)	13.0(0.7)	20.6(0.7)	7.9
W	INAA	3.4(0.2)	8.6(1.6)	16(2)	24(2)	7.1
Mo	INAA	9.1(2.5)	28(1.4)	40(5)	50(9)	5.5
Ga	INAA	43(12)	116(52)	140(23)	178(90)	4.1
Pb	AAS	73(3)	169(2)	226(4)	278(3)	3.8
V	INAA	86(44)	178(17)	244(18)	327(40)	3.8
U	INAA	8.8(1.9)	16(3)	22(4)	29(4)	3.3
Cr	AAS	28(3)	54(3)	66(3)	71(4)	2.5
Ba(%)	AAS	0.168(0.001)	0.245(0.002)	0.320(0.013)	0.409(0.018)	2.4
Cu	AAS	56(1)	89(1)	107(4)	137(1)	2.4
Be	AAS	6.5(0.2)	8.5(0.2)	9.5(0.3)	10.3(0.5)	1.6
Mn	AAS	209(7)	231(5)	273(7)	309(3)	1.5
Si(%)	AAS	29.6(0.7)	28.0(0.1)	27.5(0.3)	26.8(0.1)	0.90

¹Concentration dependence with particle size was determined qualitatively with the criteria that consistent concentration trends beyond experimental uncertainty were observed for each fraction.

²Ratio of concentration in Fraction 4 to that in Fraction 1.

³AAS values are the averages of two independent determinations; the ranges are given in parentheses. ⁴INAA values are the largest of twice the weighted standard deviation, the range, or an estimate of the accuracy.

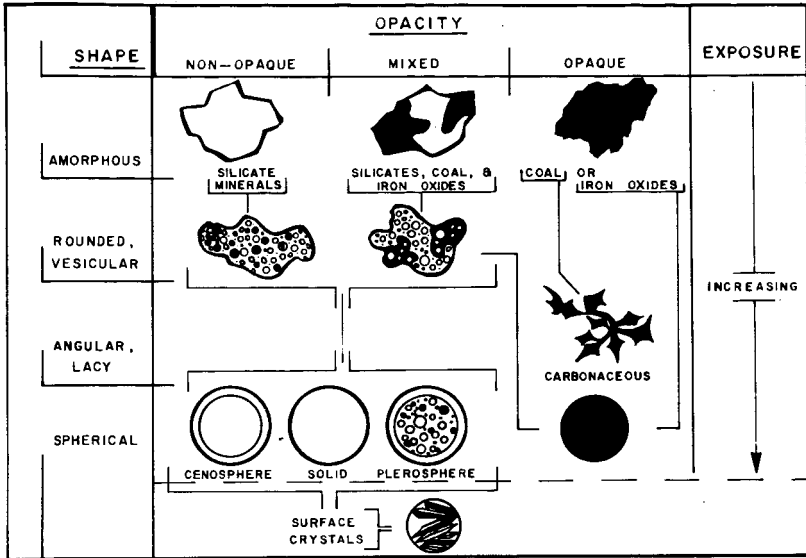


Fig. 1. Fly ash morphogenesis scheme illustrating probable relationship of opacity and shape to particle composition and exposure in the combustion chamber.